Genome-wide binding map of the histone deacetylase Rpd3 in yeast

Siavash K. Kurdistani[1,2], Daniel Robyr[1], Saeed Tavazoie[3] & Michael Grunstein[1]

Published online: 24 June 2002, doi:10.1038/ng907

We describe the genome-wide distribution of the histone deacetylase and repressor Rpd3 and its associated proteins Ume1 and Ume6 in *Saccharomyces cerevisiae*. Using a new cross-linking protocol, we found that Rpd3 binds upstream of many individual genes and upstream of members of gene classes with similar functions in anabolic processes. In addition, Rpd3 is preferentially associated with promoters that direct high transcriptional activity. We also found that Rpd3 was absent from large sub-telomeric domains. We show by co-immunoprecipitation and by the high similarity of their binding maps that Ume1 interacts with Rpd3. In contrast, despite the known role of Ume6 in Rpd3 recruitment, only a limited number of the genes targeted by Rpd3 are also enriched for (or targeted by) Ume6. This suggests that Rpd3 is brought to many promoters by alternative recruiters, some of which may bind the putative *cis*-regulatory DNA elements that we have identified in sets of Rpd3 target genes. Finally, we show that comparing the genome-wide pattern of Rpd3 binding with gene expression and histone acetylation in the *rpd3Δ* mutant strain reveals new sites of Rpd3 function.

Introduction

Histone deacetylases can exert gene-specific repression of transcription when recruited by a DNA-binding protein to particular genomic loci[1,2]. For instance, Ume6 binds to the URS1 element of the *INO1* promoter and recruits the Rpd3 complex, by means of the Sin3 co-repressor, to deacetylate approximately two adjacent nucleosomes, with a resulting repression of transcription[2–4]. Despite this targeted recruitment, Rpd3 also deacetylates large regions of chromatin, including promoters and coding regions that do not contain Ume6-binding sites, in a process termed 'global deacetylation'[5]. Like local deacetylation of single genes, global deacetylation by Rpd3 represses transcription, but functions over larger chromosomal domains. Assessing the role of Rpd3 in genome-wide regulation of transcription is further complicated by the fact that the Rpd3 complex is very large (around 1 megadalton, MD) and seems to be heterogeneous[6], suggesting that there may be site-specific utilization of certain components of the complex. Together these observations indicate that Rpd3 may act through diverse local and genome-wide mechanisms that are largely unknown. Determining these mechanisms requires a genome-wide approach to finding the variety of ways in which Rpd3 recognizes chromatin, modifies histones and regulates gene expression.

Localization of Rpd3 on a whole-genome scale *in vivo* is crucial for a comprehensive understanding of its cellular role. Genome-wide expression microarrays have provided a partial picture of the histone deacetylase function by revealing genes that are derepressed when *RPD3* is deleted[7,8]. However, a large number of genes are, paradoxically, repressed in the *rpd3Δ* mutant strain, making interpretation of expression data alone difficult because of indirect effects on various cellular processes. Moreover, deletion of *RPD3* has little effect on the transcription of many genes, despite an increase in their acetylation state. A more direct approach to elucidating the function of Rpd3 is to determine the sites of increased histone acetylation throughout the genome after loss of *RPD3* by using acetylation microarrays[9]. A global analysis of acetylation provides a functional map of Rpd3 enzymatic action and identifies target genes independent of their transcriptional status. Inferring where Rpd3 binds on the basis of acetylation data is complicated, however, by functional redundancy among deacetylases and the presence or absence of histone acetyltransferases such as Gcn5 and Esa1, which increase acetylation when Rpd3 is absent. Thus, expression and acetylation microarrays require a third and complementary tool, protein-binding microarrays, to directly identify the target sequences and provide a global binding map. We show that such a panoramic map uncovers higher-order features, such as distinct chromosomal domains or regulation of groups of genes on the basis of common function, that would be concealed in a gene-by-gene survey. A global binding map also points to the presence of hitherto undiscovered recruitment mechanisms. In addition, binding maps of other members of the large and possibly heterogeneous Rpd3 complex elucidate their limited or widespread use throughout the genome. Finally, we show that binding arrays reveal new sites of function that are not readily apparent in expression or acetylation arrays.

Departments of [1]Biological Chemistry and [2]Pathology and Laboratory Medicine, University of California School of Medicine, Los Angeles, California 90095, USA. [3]Department of Molecular Biology, Lewis Thomas Laboratories, Princeton University, Princeton, New Jersey, USA. Correspondence should be addressed to M.G. (email: mg@mbi.ucla.edu).

Results

Cross-linking of Rpd3 to chromatin

To map Rpd3 binding sites on a genome-wide scale, we first used chromatin immunoprecipitation/PCR (ChIP) of formaldehyde–cross-linked chromatin combined with microarrays[10–12]. Our initial attempts at cross-linking with formaldehyde, even for extended periods, proved inadequate for significant ChIP of Rpd3-associated DNA. To improve the efficiency, we treated the cells first with dimethyl adipimidate (DMA), a protein–protein cross-linking agent, and then with formaldehyde to cross-link a Myc-tagged Rpd3 complex to its DNA target sites *in vivo*. The use of both agents increases Rpd3 cross-linking to the *INO1* promoter by approximately 8-fold, as opposed to 1.3-fold using formaldehyde alone (Fig. 1*a*). This level of enrichment is readily detected by microarrays.

Binding of Rpd3 to promoter and global regions

Deletion of *RPD3* results in hyperacetylation not only at the *INO1* promoter, but also globally in the surrounding sequences[5]. To determine whether the effect of Rpd3 on global regions is a result of long-range deacetylation from sites of recruitment, or whether the deacetylase complex binds globally, we mapped the binding of the tagged proteins Rpd3–Myc and Ume6–Flag at *INO1* by standard ChIP with anti-tag antibodies under repressive conditions, using untagged wildtype cells as a control. We found that Ume6 binds preferentially to the URS1 sequence containing the Ume6-binding site (Fig. 1*b*)[13]. Consistent with the Ume6-targeting model[2,4], Rpd3 shows a prominent peak of binding (around eightfold more than control) coincident with Ume6 binding at the URS1. However, Rpd3 binding is not restricted to the URS1 and extends throughout surrounding sequences, showing on average around 2–2.5-fold enrichment compared with control at all sites examined over a region of 10 kb around the URS1 (Fig. 1*b*). This lower level of enrichment was reproduced in several independent experiments. Notably, the non-promoter or 'global' binding at *INO1* is independent of Ume6, because *UME6* deletion abolishes the peak of Rpd3 binding at URS1 preferentially. Thus, Rpd3 binds to non-promoter (global) regions at *INO1* in the absence of Ume6. We observed similar global binding of Rpd3 at and around *PHO5*, which lacks Ume6-binding sites (data not shown). Our results indicate that promoter-specific Rpd3 binding occurs in a background of global Rpd3 binding, and that the two interactions are mechanistically distinct.

To map Rpd3–Myc binding throughout the genome, we purified DNA from chromatin cross-linked with DMA-formaldehyde by immunoprecipitation with anti-Myc, amplified it by PCR and labeled it with either Cy3 or Cy5 fluorophores. The labeled DNA from Myc-tagged and isogenic wildtype strains was combined and hybridized to a microarray glass slide containing about 6,700 intergenic regions[9,12], or more than 6,200 open reading frames (ORFs; University Health Networks, Toronto). The intergenic regions were either between two tandem genes, two convergent genes, shared by two divergent genes, or so large that they were split into smaller regions of about 1 kb on the array. In this study, shared regions between divergent ORFs were assigned to both. All experiments were repeated at least twice from samples cross-linked separately for ChIP. We found that, throughout the genome, Rpd3 was enriched 4-fold or more compared with the untagged control at 144 promoters, 3-fold or more at 205 promoters, 2-fold or more at 749 promoters, and between 1.5-fold and 2-fold at more than 1,500 promoters (Web Fig. A online). By contrast, only two ORFs were enriched for Rpd3 binding more than 3-fold, 77 more than 2-fold and around 300 more than 1.5-fold over the untagged control. We found no correlation between Rpd3 binding at an intergenic region and its adjacent ORF (correlation coefficient $r = 0.1$; see Web Fig. A online). Thus, the high number of occupied intergenic regions indicates that Rpd3 is most highly targeted to promoters and binds to a considerably lesser extent to coding regions throughout the genome.

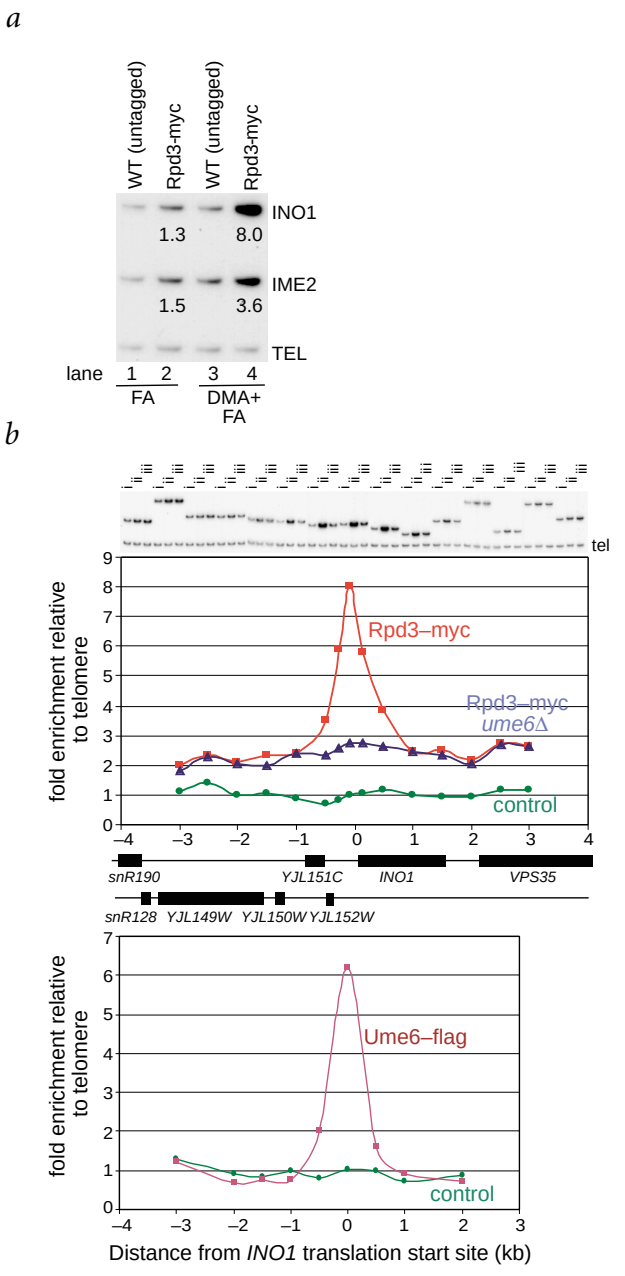

Fig. 1 Rpd3 binds to both promoter and global sites. ***a***, Serial cross-linking with DMA and formaldehyde enables more efficient chromatin immunoprecipitation of Rpd3 (compare lanes 2 and 4) at *INO1* and *IME2* promoters. The intensity of each band is normalized to a region approximately 500 bp from the end of chromosome VI-R (TEL), which is used as the internal and loading control. The fold enrichment is the ratio of the normalized values of tagged to untagged strains. FA, formaldehyde. ***b***, Binding of Rpd3 and Ume6 to the chromosomal region containing *INO1*. The graphs show relative intensity of PCR fragments normalized to the TEL band (internal control). The peaks of Rpd3 (upper panel) and Ume6 (lower panel) binding coincide with the Ume6-binding site (URS1) in the *INO1* promoter. However, Rpd3 binds to chromatin regions other than URS1 in a Ume6-independent manner. Control, untagged wild type. The location of genes in the region is shown. The standard deviation for all data points was ± ≤0.7.

Table 1 • Enrichment of Rpd3 targets for genes in functional categories

Functional category	No. of genes in category	No. of genes queried	No. of genes found	*P* value ($-\log_{10}$)
Ribosomal proteins	205	559	103	55.62
Protein synthesis	347	559	115	39.56
Organization of cytoplasm	558	559	130	27.23
rRNA processing	58	559	20	7.38
rRNA transcription	100	559	27	7.16
Amino-acid metabolism*	205	559	25	1.24
Meiosis*	101	559	13	1.00
Sporulation and germination*	110	559	9	0.20

Functional categories found among the Rpd3 target genes (≥2.5-fold enrichment) are based on the MIPS classification scheme. *P* values were calculated using the cumulative probability distribution for finding at least *k* ORFs from a particular functional category in a cluster size *n*. Because 199 MIPS categories were tested for each cluster, *P* values greater than 2.5×10^{-4} were not deemed statistically significant, as their total expectation would be greater than 0.05. *These categories are not statistically significant, but several members of each are targeted by Rpd3, consistent with the known role of Rpd3 in regulation of these pathways.

RPD3 is associated with genes of specific functional categories and high transcriptional activity

To determine whether Rpd3 regulates distinct physiological pathways, we mapped the Rpd3 target genes with 2.5-fold or more enrichment to the 199 functional categories in the MIPS functional classification database. Statistical analysis revealed that 5 of 199 functional categories were significantly enriched for genes whose upstream regions were bound by Rpd3 (Table 1)[14]. These categories include genes encoding ribosomal proteins, protein synthesis and rRNA transcription and processing. The enrichment in these specific functional categories indicates that Rpd3 may be important in the regulation of anabolic genes. Notably, categories such as 'amino-acid metabolism' ($P = 5.7 \times 10^{-2}$), 'meiosis' ($P = 1.0 \times 10^{-1}$) and 'sporulation and germination' ($P = 6.3 \times 10^{-1}$), which include some of the classical Rpd3 target genes, did not meet the statistical criterion for enrichment ($P < 2.5 \times 10^{-4}$, Table 1). Many genes in each category were enriched for Rpd3 binding, however, in agreement with previous observations that *RPD3* deletion affects such processes. In addition, Rpd3 probably influences the regulation of other cellular processes through individual genes encoding proteins such as kinases, enzymes involved in biochemical pathways and mitochondrial enzymes that are also significantly enriched for Rpd3 binding.

As Rpd3 is a repressor and has been associated with genes that are repressed in YPD medium, such as *INO1* and *IME2*, we expected that this association would hold true for most, if not all, Rpd3 target genes. Unexpectedly, actively transcribed genes, such as those encoding ribosomal proteins, have promoters that are among the most highly enriched for Rpd3 (average Rpd3 binding is around 4.5 times control). This level of Rpd3 binding occurs preferentially over the promoter and not the surrounding region. For instance, for *RPS27B* and *RPL28*, respectively, there is 2.5 and 3 times more Rpd3 at the promoters than the coding regions (data not shown). We therefore asked whether there was a statistically significant association between Rpd3 and genes with high transcriptional activity. We analyzed a published whole-genome mRNA abundance database in which the absolute number of mRNA molecules per cell is calculated when cells are grown in YPD at 30 °C (ref. 15). We found a correlation between levels of Rpd3 enrichment and the number of mRNA copies per cell (Fig. 2), indicating that Rpd3 preferentially associates with promoters such as those of ribosomal protein genes, heat-shock genes and cyclin genes, which direct high transcriptional activity.

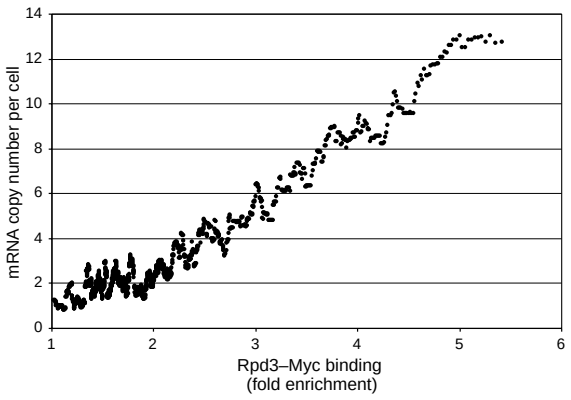

Fig. 2 Rpd3 binds preferentially to promoters that direct high transcriptional activity. The moving average (window size, 100; step size, 1) of Rpd3 enrichment immediately upstream of an ORF is plotted as a function of mRNA molecule copy number per cell.

Rpd3 binding map overlaps with Ume1 but not Ume6

The protein Ume6 is the only known DNA-binding protein that recruits the Rpd3 complex to specific loci[2,4]. We therefore examined the extent to which Rpd3 and Ume6 binding overlap at intergenic regions (Web Fig. A online). Comparing the genome-wide intergenic maps, we did not find a significant correlation between Rpd3 and Ume6 binding ($r = 0.24$; Fig. 3*c*). Only about 4% of Rpd3-bound regions (≥2.5-fold) were also enriched for Ume6 (≥1.7-fold), but around 80% of Ume6-bound regions (≥1.7-fold) were enriched for Rpd3 (≥2.5-fold). The data indicate that although Rpd3 is recruited to the bulk of Ume6 target genes, factors other than Ume6 must recruit Rpd3 to most of the deacetylase target promoters. Accordingly, Rpd3 binding at intergenic regions of the ribosomal protein genes is unaffected by deletion of *UME6* (data not shown).

As the composition of the multiprotein Rpd3 complex may be heterogeneous[6,16], a comparison of global binding of different components should distinguish essential members that are always associated with the complex on chromatin. We previously found that Ume1, which negatively regulates meiosis-specific genes[17], is associated with the Rpd3/Sin3 complex (A. Carmen, J. Wu, P. Griffin and M.G., unpublished data). To determine whether Ume1 physically interacts with Rpd3, we carried out co-immunoprecipitation experiments from whole-cell lysates treated with DNase I. Anti-hemagglutinin (HA) immunoprecipitates not only HA-tagged Ume1 (Ume1–HA) but also Rpd3 (Fig. 3*a*). Conversely, anti-Rpd3 immunoprecipitates both Rpd3 and Ume1–HA. In addition, the pattern of Ume1 binding at specific loci such as *INO1* (Fig. 3*b*) and *PHO5* (data not shown) is highly similar to Rpd3 binding. Finally, when we compared the genome-wide distribution of Ume1 and Rpd3, we found that their binding maps are highly overlapping ($r = 0.80$, Fig. 3*c*). We therefore conclude that Ume1 is associated with the Rpd3 complex at most, if not all, sites throughout the genome. Deletion of *UME1* does not affect targeted or global Rpd3 binding (data not shown). However, there is a slight increase (roughly 1.5-fold) in histone

tail acetylation as measured on histone H4 lysine 12 (H4K12), in the *ume1Δ* strain compared with the wild type, indicating that Ume1 is weakly required for the full deacetylase activity of the Rpd3 complex.

Rpd3 targets promoters with specific DNA sequence motifs

To identify *cis*-regulatory elements that may contribute to targeting Rpd3, we applied the Gibbs sampling algorithm, implemented in the AlignACE program[18], to find candidate regulatory motifs in DNA upstream of target genes of Rpd3, Ume6 and Ume1. We found 34 motifs that passed our criteria for potential biological significance (Table 2; Methods). As expected, motif 1, which emerged from Rpd3, Ume1 and Ume6 target genes, was identified as URS1. This motif was only found among genes with an intermediate level of Rpd3 enrichment, indicating that the top 200 genes or so that are highly enriched for Rpd3 use a recruiting mechanism other than Ume6. Motifs 2–6 were specific to Rpd3 and Ume1 target genes, but not to those of Ume6. Motif 2 was identified as the Rap1-binding site, which is known to be upstream of many ribosomal protein genes and is required for recruiting Esa1 acetyltransferase[19]. Whether Rap1 also helps to recruit Rpd3 has yet to be established. Motifs 3 and 4 were previously identified as M3a and M3b and were shown to have high specificity for genes in an 'RNA metabolism and translation' cluster that was defined on the basis of a common expression pattern across the cell cycle[14]. Although M3a and M3b motifs have not been characterized experimentally, their high specificity indicates that they may be involved in the global regulation of protein synthesis[14]. Motifs 5–8 were not previously identified experimentally or computationally, but may contribute to co-regulation of certain Rpd3 target genes. We conclude that sequences other than URS1 are likely to recruit Rpd3 to most promoters examined.

Rpd3 is excluded from telomeric and sub-telomeric domains

To identify chromosomal domains throughout which Rpd3 is found or from which it is excluded, we sorted intergenic regions into groups of 50 according to their average distance from their closest telomere. The fraction of regions with Rpd3 enrichment of 1.5-fold or more compared with the control in each group was then plotted against their average distance from a telomere (Fig. 4)[20]. We found that at distances up to 20 kb from the telomere, only about 25% and 5% of regions were bound by Rpd3 at 1.5-fold and 2-fold or greater than control, respectively (see Fig. 4 and Web Fig. A online). For the whole genome, on average, significant Rpd3 enrichment occurred at 40 kb or farther from telomeres where 20% of intergenic regions showed twofold or greater enrichment for Rpd3 binding (see Web Fig. A online). Thus, there is a relative absence of Rpd3 binding more proximal to the telomeres. It has been shown that large regions in the sub-telomeric domains are maintained in a repressive state by Tup1 repressor/Hda1 histone deacetylase[9]. Such repressed domains may physically exclude Rpd3 by generating a specialized form of chromatin that extends much farther than the telomeric heterochromatin[21].

Rpd3 binding is complementary to acetylation and expression arrays

We sought to determine the relationship between genome-wide binding of Rpd3 in wildtype cells and the genome-wide acetylation[9] and expression[8] resulting from the absence of Rpd3 in the deletion mutant *rpd3Δ*. When the level of Rpd3 binding was plotted as a function of acetylation of histone H3 lysine 18 (H3K18) for intergenic regions, we found that the chromosomal sites that were highly acetylated in the absence of Rpd3 tended to be those highly enriched for Rpd3 binding (Fig. 5*a*). This genome-wide tendency is similar to the findings for URS1 in the *INO1* promoter region[4]. However, among genes whose upstream regions are the most enriched for Rpd3 binding is a large group (approximately 130 genes) encoding ribosomal proteins that show no significant increase in histone tail acetylation[9] or expression when *RPD3* is deleted[7,8]. This is reflected in the decrease in the correlation of binding with hyperacetylation at these higher levels of Rpd3 enrichment (Fig. 5*a*). When the same data excluding ribosomal protein genes were plotted, we found a significant association between Rpd3 binding and *rpd3Δ*-mediated acetylation for H3K18 (Fig. 4*a*) as well as H3K9, H4K12 and H4K16 (data not shown) across the intergenic regions throughout the genome. Comparison

Table 2 • DNA sequence motifs found among the Rpd3 target genes

Sequence logo	Motif	MAP score	Group specificity (*P* value)
1	URS1	120	8.2×10^{-3}
2	RAP1	72	1.7×10^{-17}
3	M3a	67	6.2×10^{-10}
4	M3b	67	8.8×10^{-16}
5	unknown	17	1.6×10^{-21}
6	unknown	3.1	1.2×10^{-14}
7	unknown	2.7	1.8×10^{-9}
8	unknown	10	2.3×10^{-17}

Sequence logo representation of the motifs discovered in Rpd3, Ume1 and Ume6 target genes. The overall height of the stack reflects positional information content of the sequence (0–2 bits). The height of each letter is proportional to its frequency, with the most frequent on top. The MAP score is an AlignAce internal metric used to determine the significance of an alignment. Group specificity is a measure of the significance of association of a motif with the cluster in which it was found versus the entire genome.

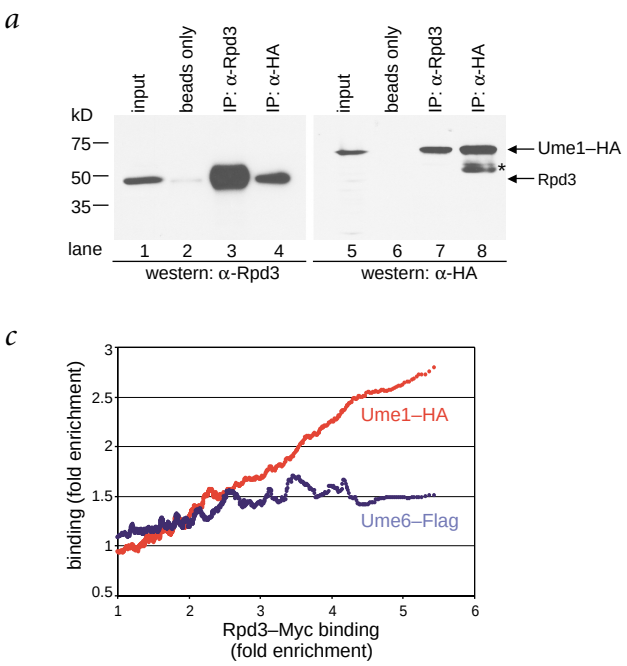

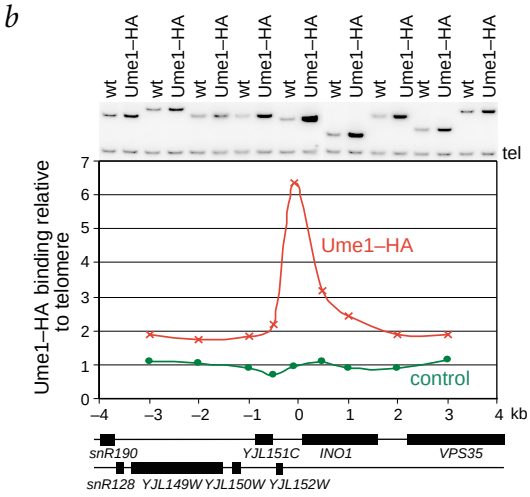

Fig. 3 Ume1 is a newly discovered member of the Rpd3 complex in yeast. ***a***, Ume1–HA and Rpd3 co-immunoprecipitate (lanes 4 and 7) from whole-cell extracts. The asterisk denotes partially degraded Ume1–HA. ***b***, ChIP analysis of Ume1–HA binding at and around *INO1*. Ume1 binding at *INO1* is similar to that of Rpd3, showing both promoter-specific (over URS1) as well as global binding. wt, wild type. ***c***, Genome-wide binding of Rpd3 correlates with that of Ume1 but not of Ume6.

of binding with expression in the *rpd3Δ* strain also revealed preferential association of Rpd3 with genes that are most derepressed in *rpd3Δ*, except for the group of ribosomal protein genes (Fig. 5*b* and data not shown). These data show that the binding array uniquely identifies Rpd3 as a potential regulator of ribosomal protein genes, a finding that would be altogether missed by the acetylation or expression arrays. Notably, when comparing Rpd3 binding with gene expression in *sin3Δ* mutants, we found a better correlation between levels of Rpd3 binding and derepression when *SIN3* was deleted than when *RPD3* was deleted (Fig. 5*b*). As deletion of *SIN3* leads to loss of Rpd3 binding at promoters as well as globally (data not shown), these data indicate that Sin3 remains bound to Rpd3 target genes when *RPD3* is deleted and are consistent with previous findings that Sin3 can repress transcription independent of Rpd3 (ref. 22). Thus, binding arrays not only confirm the expression and acetylation data but also complement them by revealing sites of Rpd3 function that are hidden in the other arrays.

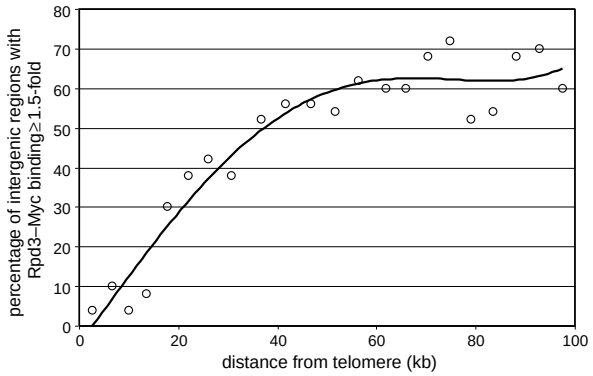

Fig. 4 Rpd3 is excluded from telomeric and sub-telomeric regions. Intergenic regions were sorted in groups of 50 according to the average distance from their closest telomere end for the first 100 kb, to avoid overlap between two ends of a chromosome. The fraction of regions with Rpd3 enrichment greater than or equal to 1.5 times that of the control in each group was then plotted against their average distance from a telomere.

Discussion

We have used a modified cross-linking method for ChIP that includes a protein–protein cross-linking agent in addition to formaldehyde. This allowed us to map Rpd3 binding in yeast for the first time. The genome-wide binding maps of Rpd3 and its associated factor Ume1 show that the histone deacetylase complex is common to a large and diverse set of promoters. Within this set, Rpd3 probably regulates whole gene classes (for example, ribosomal protein genes) by binding to the promoters of their member genes. At most loci, Rpd3 targeting occurs independently of Ume6, the only known recruiter of Rpd3 in yeast. We also show that Rpd3 binds globally to non-promoter sequences using a mechanism that is also independent of Ume6 recruitment. Thus, our data exclude a Ume6-dependent 'initiation and spreading' mechanism, but indicate that other recruitment factors and DNA motifs are involved in bringing Rpd3 to most promoters that are enriched for this deacetylase. In contrast to targeted loci, the Rpd3 complex may bind directly and in a sequence-independent manner to histones or histone-binding proteins for global deacetylation[5].

Notably, Rpd3, a known repressor of transcription, associates preferentially with the upstream regions of genes that direct high transcriptional activity. This indicates that the recruitment of the deacetylase complex to a promoter alone is insufficient for repression, and subsequent events may be required for the Rpd3 complex to repress transcription. Such events could involve post-translational modifications of the Rpd3 complex or conditional association of other members of the Rpd3 complex, such as Sap30, Sds3 and Pho23, which affect its deacetylase activity[23–25]. In such a scheme, the Rpd3 complex would be poised for rapid and effective repression of highly active genes when needed at a later stage. This may be the case for the ribosomal protein genes. Although *RPD3* deletion has no effect on ribosomal protein gene expression in exponentially growing cells[7,8], the *rpd3Δ* mutant does not undergo the temporal changes in expression of ribosomal protein genes at the diauxic transition that occurs in the wildtype

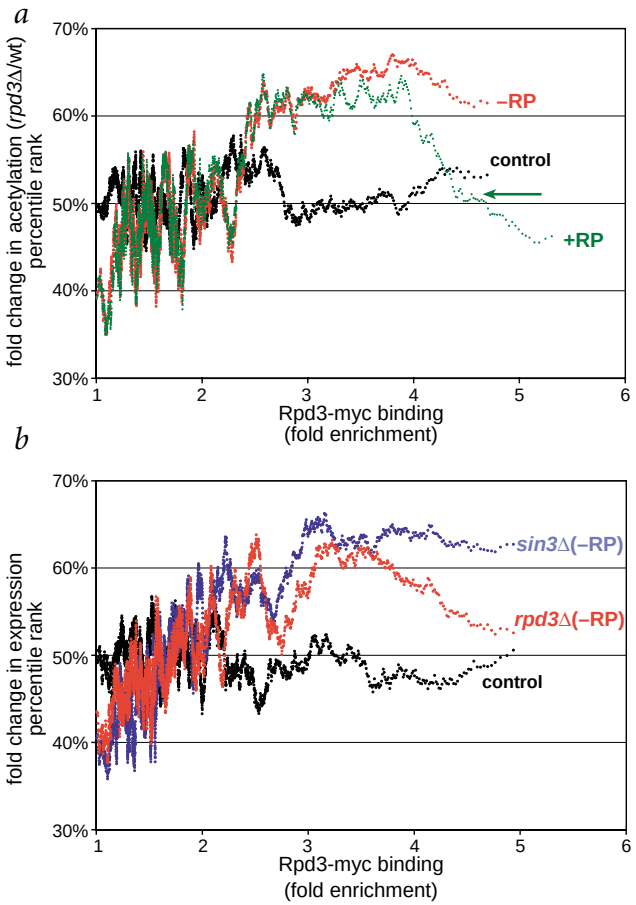

Fig. 5 Rpd3 binding is complementary to acetylation and expression arrays. ***a***, Moving average (window size, 100; step size, 1) of Rpd3 enrichment over intergenic regions is plotted as a function of percentile rank of histone H3 lysine 18 (H3K18) acetylation in *rpd3Δ*: including ribosomal protein genes (green, +RP, arrow); excluding ribosomal protein genes (red, –RP); control IP (black). ***b***, Moving average (window size, 100; step size, 1) of Rpd3 enrichment over intergenic regions is plotted as a function of percentile rank of fold change in expression in *rpd3Δ* (red) or *sin3Δ* (blue) mutants. The data for ribosomal protein genes are excluded for clarity. Percentile rank reflects the relative standing of values in a data set.

cells (S.K.K., V. Iyer, P.O. Brown and M.G., unpublished data). Moreover, because acetylation has been associated with active transcription[26,27], more deacetylase activity (hence more Rpd3) may be needed to counteract the increased acetyltransferase activity at heavily transcribed genes. This is also consistent with observations that the acetyl groups in the four core histones have a short turnover time[28]. Association of Rpd3 with highly transcribed genes may also explain why Rpd3 is excluded from the intergenic regions of genes in large subtelomeric domains. These domains of about 20–25 kb are transcriptionally silenced by Tup1/Hda1 in YPD medium[9], and thus the need for an Rpd3-mediated reversal of acetylation associated with transcription may be obviated. The pattern of Rpd3 binding to *Drosophila melanogaster* salivary gland polytene chromosomes, as determined by immunofluorescence staining, reveals widespread binding of this complex to repressed euchromatic interbands[29]. Whether this represents an organismal difference or differences in the resolution of the two procedures has yet to be determined.

The localization of Rpd3 to specific chromosomal loci can now be used to delineate the direct effects of a deletion of *RPD3* (*rpd3Δ*) from those that are indirect and to define the role of various members of the Rpd3 complex in its binding to chromatin. This latter point is underscored by our finding that Ume1 is closely correlated with Rpd3 both at promoters and globally but has no effect on Rpd3 binding and only a minor effect on the deacetylase activity *in vivo*. In contrast, Ume6, whose absence gives an overlapping phenotype with that of *rpd3Δ*, is only required for Rpd3 localization at a limited number of promoters. Application of this approach to other members of the complex should provide insights into how the Rpd3 complex regulates gene expression.

Methods

Cross-linking and immunoprecipitation. All washes are with ice-cold 1 × PBS. For Rpd3–Myc and Ume1–HA, 50 ml yeast cells, grown to $O.D_{600}$ ~ 0.8 in YEPD medium, were washed twice and resuspended in ice-cold 10 mM DMA (Pierce) and 0.25% DMSO in PBS for 45 min at room temperature on a nutator. Cells were then washed twice and resuspended in 1% formaldehyde in PBS for approximately 11 h at room temperature. We found that DMA alone or shorter formaldehyde treatment is insufficient for cross-linking Rpd3 to chromatin, and that 11 h of formaldehyde cross-linking achieves a balance between maximal enrichment and efficient shearing of chromatin (average fragment size ~400 bp). We then carried out ChIP essentially as described[5]. We cross-linked Ume6–Flag with formaldehyde for 15 min at room temperature and then carried out ChIP as described[13]. The results from cross-linking of Ume6–Flag with DMA and formaldehyde (as above) were indistinguishable from those obtained with formaldehyde alone. All antibodies were monoclonal—anti-Myc (9E10), anti-HA (HA.11) or anti-Flag (M2) (Covance)—except for anti-Rpd3 (Upstate Biotechnology; rabbit polyclonal). We used 1/100 of immunoprecipitated DNA for analysis by PCR in the presence of 0.8 μCi μl^{-1} [γ-^{32}P]dATP. We quantified the data using the PhosphorImager. For microarray studies, we amplified 15% of the immunoprecipitated DNA and fluorescently labeled it by Klenow random priming (Gibco/BRL) as described at the microarrays.org website listed below. For Ume1–HA and Rpd3 co-immunoprecipitation, we produced whole-cell lysates (from 50 ml culture, $O.D_{600}$ ~0.8) using glass beads and subjected them to DNase I treatment (10 U/100 μl lysate) for 15 min at 37 °C. Appropriate antibodies or beads alone were added, the mixture was incubated at 4 °C for 1 h and 50 μl of 50% protein A suspension was added for another hour. The beads were washed extensively with buffers including 500 mM NaCl and 0.25 M LiCl/0.5% NP-40/0.5% sodium deoxycholate. We then boiled the beads in SDS loading buffer and subjected them to standard SDS–PAGE and western blotting.

DNA microarray, hybridization and analysis. Primer pairs (Research Genetics) were designed to amplify approximately 6,700 intergenic regions from yeast genomic DNA by PCR as described and selected for size and purity by agarose gel electrophoresis[9,12]. We resuspended amplified sequences in 3 × SSC and printed them on aminosilane-coated slides (Corning) using a microarrayer built as indicated at the MGuide v. 2.0 website. We obtained yeast ORF (coding region) microarrays from University Health Networks, Toronto. Fluorescent probes were mixed, purified, concentrated through a microcon-30 filter (Amicon) and hybridized overnight to microarrays in 5 × SSC, 50% formamide, 0.2% SDS, 0.5 mg ml^{-1} tRNA and 0.5 mg ml^{-1} salmon sperm at 44 °C in a humid chamber. Microarrays were briefly washed in 2 × SSC to remove the coverslip. We then washed the slides at room temperature for 5 min in 0.1 × SSC/0.1% SDS and twice in 0.1 × SSC. We scanned microarrays (GMS 418 Array Scanner, Genetic Micro Systems) and quantified fluorescence intensities using Imagene software v. 4.1 (BioDiscovery). The data for all experiments were normalized against intensities at telomere 6R. Normalization with total intensity produced similar results.

Searching for upstream regulatory motifs. We used the AlignACE algorithm, as described previously[14,18], to conduct a search for DNA sequence motifs upstream of target genes of Rpd3, Ume6 and Ume1. Our initial search identified 665 motifs, which were subsequently clustered at a CompareACE score of 0.9 (ref. 18). The top 34 motifs with MAP score above 2.5 and specificity score above 10^{-5} were chosen as biologically significant.

Strains. We generated the Rpd3–Myc strain (SKY104) through transformation of the linearized (*Bgl*II) pRPD3-4 plasmid containing *RPD3* fused to multiple copies of the *MYC* epitope encoding sequence into the wildtype YDS2 strain. We generated the Ume1–HA strain (SKY112) by PCR-based tagging of the 3′ end of *UME1* in the chromosomal locus through homologous recombination using the pYM3 plasmid as described[13,30]. Ume6–Flag (YTT900) and its isogenic wildtype strain (YTT0166) were gifts from T. Tsukiyama[13].

URLs. MIPs classification database (Protfam), http://mips.gsf.de; microarrays.org, http://www.microarrays.org; The MGuide v. 2.0, http://cmgm.stanford.edu/pbrown/mguide. Supplemental data, including Ume1 and Ume6, and the 34 motifs, is hosted at http://www.uclaaccess.ucla.edu/labs/grunstein/Rpd3_binding.html.

Note: Supplementary information is available on the Nature Genetics website.

Acknowledgments

We are grateful to P.O. Brown for providing the primer sets for the intergenic arrays and to the laboratory of S. Nelson for use of their microarray scanner. We also thank T. Tsukiyama for providing yeast strains and plasmids for PCR-based tagging, I. Xenarios for help with data analysis, J.S. Wu for help with co-immunoprecipitation experiments and members of the Grunstein laboratory for discussions throughout this work. S.K.K. is a Howard Hughes Medical Institute Physician Postdoctoral Fellow. D.R. is a recipient of fellowships from the Swiss National Science Foundation and the Roche Research Foundation. This work was supported by Public Health Service grants from the National Institutes of Health (to M.G.).

Competing financial interests statement

The authors declare that they have no competing financial interests.

Received 9 January; accepted 14 May 2002.

1. Wu, J., Suka, N., Carlson, M. & Grunstein, M. TUP1 utilizes histone H3/H2B-specific HDA1 deacetylase to repress gene activity in yeast. *Mol. Cell* **7**, 117–126 (2001).
2. Kadosh, D. & Struhl, K. Repression by Ume6 involves recruitment of a complex containing Sin3 corepressor and Rpd3 histone deacetylase to target promoters. *Cell* **89**, 365–371 (1997).
3. Kadosh, D. & Struhl, K. Targeted recruitment of the Sin3-Rpd3 histone deacetylase complex generates a highly localized domain of repressed chromatin *in vivo*. *Mol. Cell. Biol.* **18**, 5121–5127 (1998).
4. Rundlett, S.E., Carmen, A.A., Suka, N., Turner, B.M. & Grunstein, M. Transcriptional repression by UME6 involves deacetylation of lysine 5 of histone H4 by RPD3. *Nature* **392**, 831–835 (1998).
5. Vogelauer, M., Wu, J., Suka, N. & Grunstein, M. Global histone acetylation and deacetylation in yeast. *Nature* **408**, 495–498 (2000).
6. Kasten, M.M., Dorland, S. & Stillman, D.J. A large protein complex containing the yeast Sin3p and Rpd3p transcriptional regulators. *Mol. Cell. Biol.* **17**, 4852–4858 (1997).
7. Bernstein, B.E., Tong, J.K. & Schreiber, S.L. Genomewide studies of histone deacetylase function in yeast. *Proc. Natl Acad. Sci. USA* **97**, 13708–13713 (2000).
8. Hughes, T.R. *et al.* Functional discovery via a compendium of expression profiles. *Cell* **102**, 109–126 (2000).
9. Robyr, D. *et al.* Microarray deacetylation maps determine genomewide functions for yeast histone deacetylases. *Cell* **109**, 437–446 (2002).
10. Lieb, J.D., Liu, X., Botstein, D. & Brown, P.O. Promoter-specific binding of Rap1 revealed by genome-wide maps of protein–DNA association. *Nature Genet.* **28**, 327–334 (2001).
11. Ren, B. *et al.* Genome-wide location and function of DNA-binding proteins. *Science* **290**, 2306–2309 (2000).
12. Iyer, V.R. *et al.* Genomic binding sites of the yeast cell-cycle transcription factors SBF and MBF. *Nature* **409**, 533–538 (2001).
13. Goldmark, J.P., Fazzio, T.G., Estep, P.W., Church, G.M. & Tsukiyama, T. The Isw2 chromatin remodeling complex represses early meiotic genes upon recruitment by Ume6p. *Cell* **103**, 423–433 (2000).
14. Tavazoie, S., Hughes, J.D., Campbell, M.J., Cho, R.J. & Church, G.M. Systematic determination of genetic network architecture. *Nature Genet.* **22**, 281–285 (1999).
15. Holstege, F.C. *et al.* Dissecting the regulatory circuitry of a eukaryotic genome. *Cell* **95**, 717–728 (1998).
16. Rundlett, S.E. *et al.* HDA1 and RPD3 are members of distinct yeast histone deacetylase complexes that regulate silencing and transcription. *Proc. Natl Acad. Sci. USA* **93**, 14503–14508 (1996).
17. Pemberton, L.F. & Blobel, G. Characterization of the Wtm proteins, a novel family of *Saccharomyces cerevisiae* transcriptional modulators with roles in meiotic regulation and silencing. *Mol. Cell. Biol.* **17**, 4830–4841 (1997).
18. Hughes, J.D., Estep, P.W., Tavazoie, S. & Church, G.M. Computational identification of *cis*-regulatory elements associated with groups of functionally related genes in *Saccharomyces cerevisiae*. *J. Mol. Biol.* **296**, 1205–1214 (2000).
19. Reid, J.L., Iyer, V.R., Brown, P.O. & Struhl, K. Coordinate regulation of yeast ribosomal protein genes is associated with targeted recruitment of Esa1 histone acetylase. *Mol. Cell* **6**, 1297–1307 (2000).
20. Wyrick, J.J. *et al.* Chromosomal landscape of nucleosome-dependent gene expression and silencing in yeast. *Nature* **402**, 418–421 (1999).
21. Renauld, H. *et al.* Silent domains are assembled continuously from the telomere and are defined by promoter distance and strength, and by SIR3 dosage. *Genes. Dev.* **7**, 1133–1145 (1993).
22. Laherty, C.D. *et al.* Histone deacetylases associated with the mSin3 corepressor mediate mad transcriptional repression. *Cell* **89**, 349–356 (1997).
23. Loewith, R. *et al.* Pho23 is associated with the Rpd3 histone deacetylase and is required for its normal function in regulation of gene expression and silencing in *Saccharomyces cerevisiae*. *J. Biol. Chem.* **276**, 24068–24074 (2001).
24. Lechner, T. *et al.* Sds3 (suppressor of defective silencing 3) is an integral component of the yeast Sin3·Rpd3 histone deacetylase complex and is required for histone deacetylase activity. *J. Biol. Chem.* **275**, 40961–40966 (2000).
25. Laherty, C.D. *et al.* SAP30, a component of the mSin3 corepressor complex involved in N-CoR-mediated repression by specific transcription factors. *Mol. Cell* **2**, 33–42 (1998).
26. Orphanides, G. & Reinberg, D. RNA polymerase II elongation through chromatin. *Nature* **407**, 471–475 (2000).
27. Wittschieben, B.O. *et al.* A novel histone acetyltransferase is an integral subunit of elongating RNA polymerase II holoenzyme. *Mol. Cell* **4**, 123–128 (1999).
28. Waterborg, J.H. Dynamics of histone acetylation in *Saccharomyces cerevisiae*. *Biochemistry* **40**, 2599–2605 (2001).
29. Pile, L.A. & Wassarman, D.A. Chromosomal localization links the SIN3-RPD3 complex to the regulation of chromatin condensation, histone acetylation and gene expression. *EMBO J.* **19**, 6131–6140 (2000).
30. Gelbart, M.E., Rechsteiner, T., Richmond, T.J. & Tsukiyama, T. Interactions of Isw2 chromatin remodeling complex with nucleosomal arrays: analyses using recombinant yeast histones and immobilized templates. *Mol. Cell. Biol.* **21**, 2098–2106 (2001).